PNAS
www.pnas.org

Supplementary Information for:

Structure of Ycf1p reveals the transmembrane domain TMD0 and the regulatory region of ABCC transporters

Sarah C. Bickers[a,b], Samir Benlekbir[c], John L. Rubinstein[c,d,e], Voula Kanelis[a,b,f]

Corresponding authors

Voula Kanelis
Email: voula.kanelis@utoronto.ca

John Rubinstein
Email: john.rubinstein@utoronto.ca

This PDF file includes:
Figs. S1 to S9
Table S1
References for supplementary information

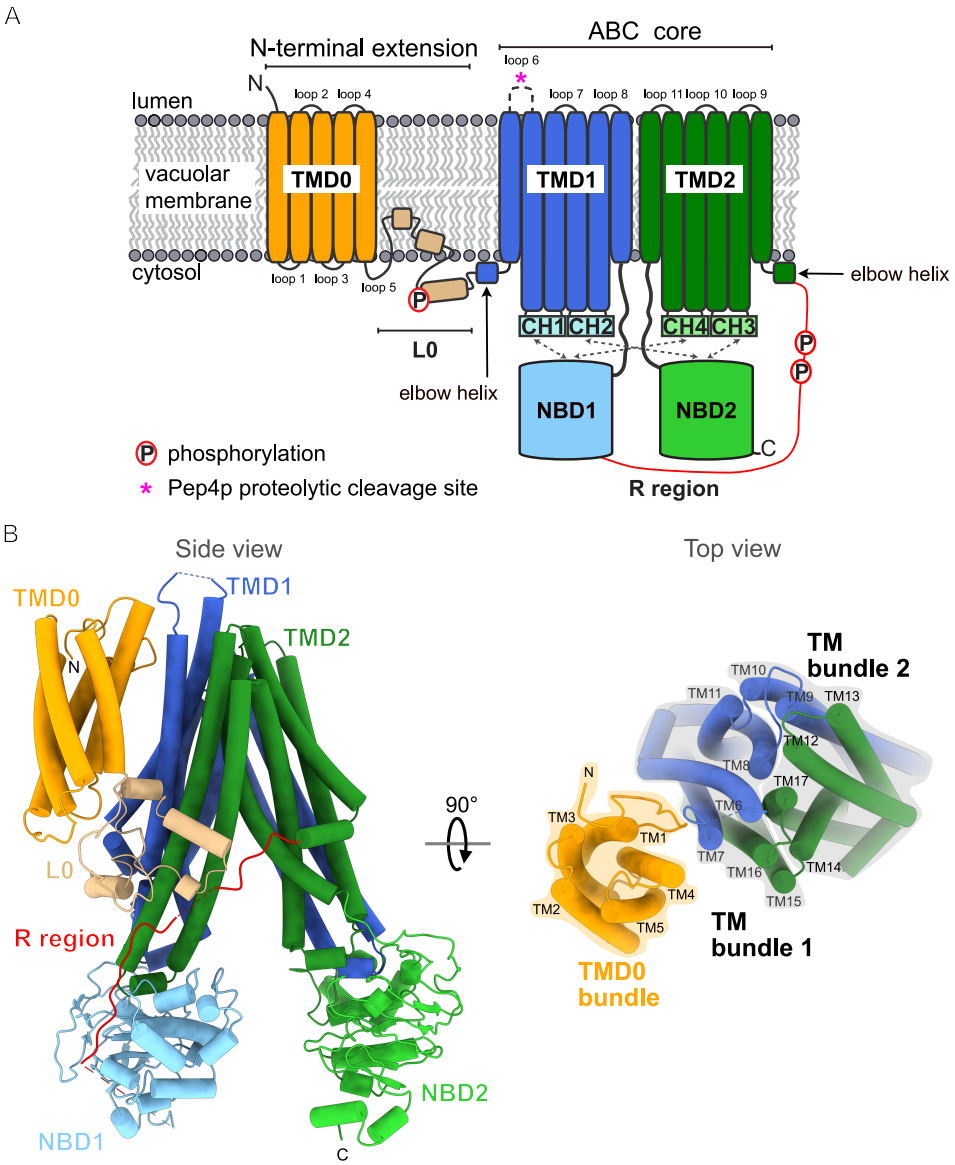

Fig. S1. Domain architecture and post-translational modifications in Ycf1p. (A) Cartoon representation of Ycf1p in the vacuolar membrane showing the two transmembrane domains (TMD1 in dark blue and TMD2 in dark green), two nucleotide binding domains (NBD1 in light blue and NBD2 in light green), and regulatory (R) region (red) that comprise the ABC core. Coupling helices (CH1, CH2, CH3, CH4) that connect the cytoplasmic extensions of the transmembrane (TM) helices in TMD1 and TMD2 are also shown, with CH1 and CH2 in pale blue, and CH3 and CH4 in pale green. The elbow helices of TMD1 and TMD2 are shown in blue and green, respectively. The N-terminal extension of Ycf1p is formed by TMD0 (orange) and L0 linker (tan). Loops, either in the lumen or cytosol, are labeled sequentially. Loop 6, which is proteolytically cleaved, is depicted as a dashed curve with a pink asterisk highlighting the proteolysis site. Phosphorylation sites in the L0 linker (S251) and R region (S908 and T911) are depicted with a red-encircled " P ". (B) Schematic diagram of the Ycf1p cryo-EM structure with cylinders representing α-helices and arrows representing β-strands. The top view, which is from the luminal side, highlights the composition and orientation of the TMD0 bundle (TM helices 1-5), TM bundle 1 (TM helices 6,7,8,11,15,16), and TM bundle 2 (TM helices 9,10,12,13,14,17).

A

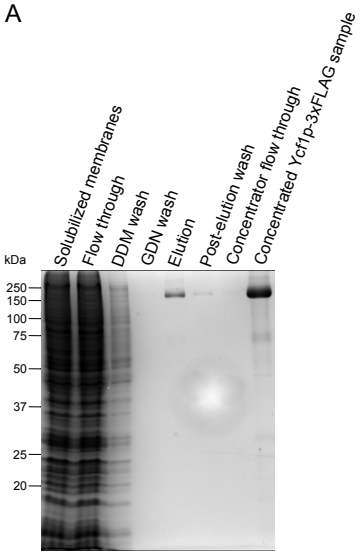

B

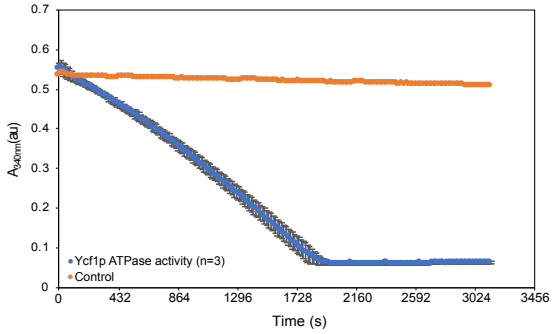

C

	Number of Fragments Detected by LC-MS/MS	
Residue	**Non-Phosphorylated**	**Phosphorylated**
S251	154	12
S488	215	2
S863	136	6
S869	104	38
S870	128	14
S872	96	46
S873	101	41
S877	172	13
S878	162	26
S899	362	2
S903	101	263
S908	25	131
T911	33	123
S914	69	88
S1126	200	1
S1313	34	1

Fig. S2. Ycf1p sample preparation. (A) 12% sodium dodecyl sulphate–polyacrylamide gel electrophoresis (SDS-PAGE) gel of a purification of Ycf1p-3×FLAG sample (171 kDa). (B) ATPase activity of Ycf1p. Blue circles indicate the mean value with error bars showing ± s.d. (n=3 assays) for absorbance at 340 nm, which follows oxidation of NADH in an enzyme-coupled assay. The control sample includes all components in the NADH enzyme-coupled ATPase assay without Ycf1p. (C) Table displaying number of fragments from phosphorylated and non-phosphorylated peptide covering the indicated residues, as detected by LC-MS/MS. Briefly, purified Ycf1p was reduced (using DTT) and treated with iodoacetate to alkylate Cys residues prior to trypsin digestion overnight. The sample was desalted and concentrated prior to LC-MS/MS analysis. A total of 0.47 µg of the digested Ycf1p sample was used.

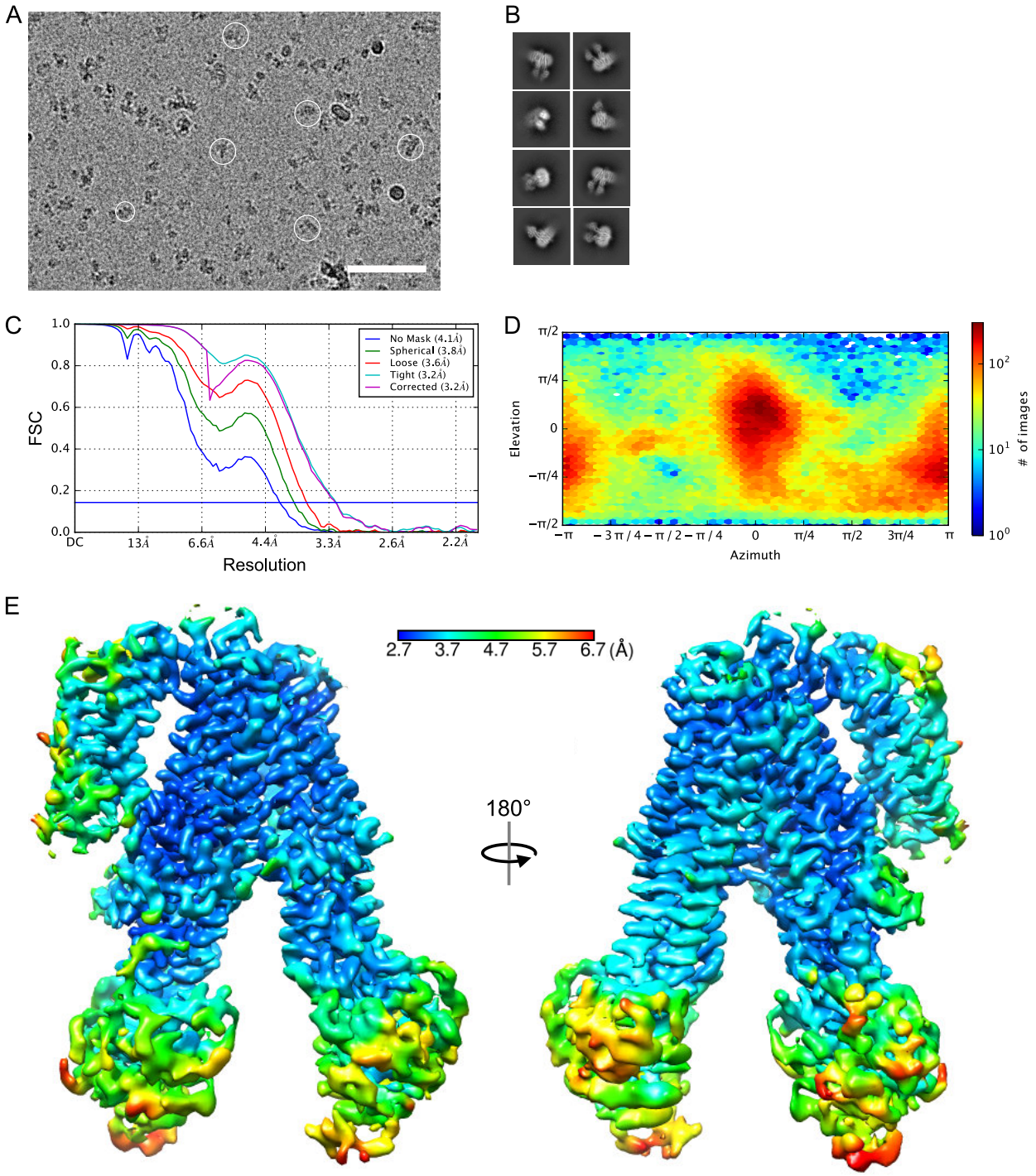

Fig. S3. Cryo-EM image analysis. (A) Section of a representative micrograph with example Ycf1p particles circled in white. Scale bar, 500 Å. (B) Example 2D class average images of Ycf1p. (C) Fourier Shell Correlation (FSC) curve for the Ycf1p map. (D) Euler angle distribution for particle images contributing to the map. (E) Local resolution estimated for the Ycf1p map.

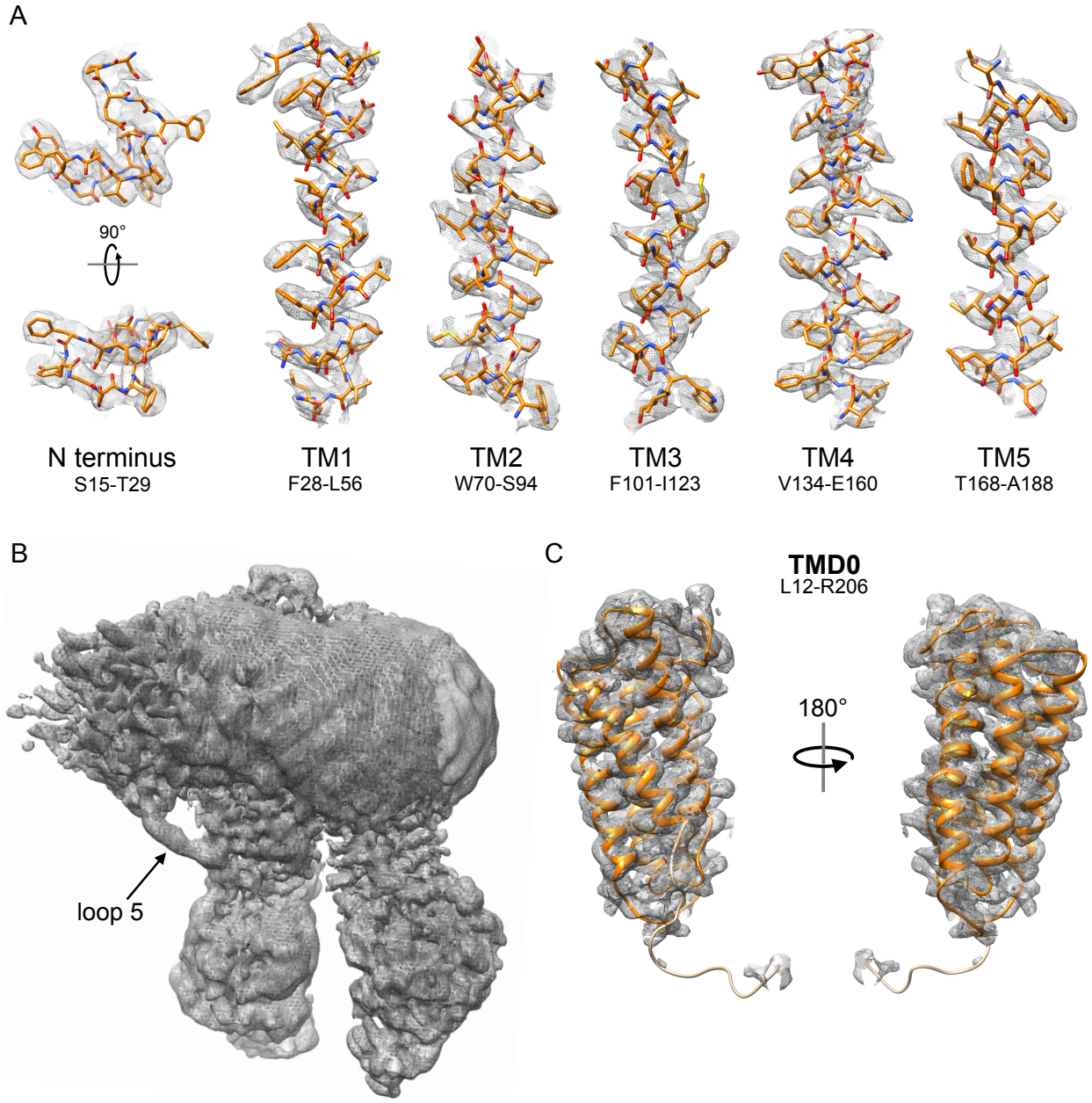

Fig. S4. Atomic model of TMD0. (A) Fitting of the luminal N-terminal tail and individual TMD0 helices (TM1 to TM5) into the cryo-EM density. (B) Low-resolution density corresponding to cytosolic loop 5 (L186-R206), which connects TMD0 and the membrane embedded region of the L0 linker, is seen consistently when maps of Ycf1p are rendered at a low-density cutoff. (C) Model of TMD0 fit into experimental cryo-EM density map.

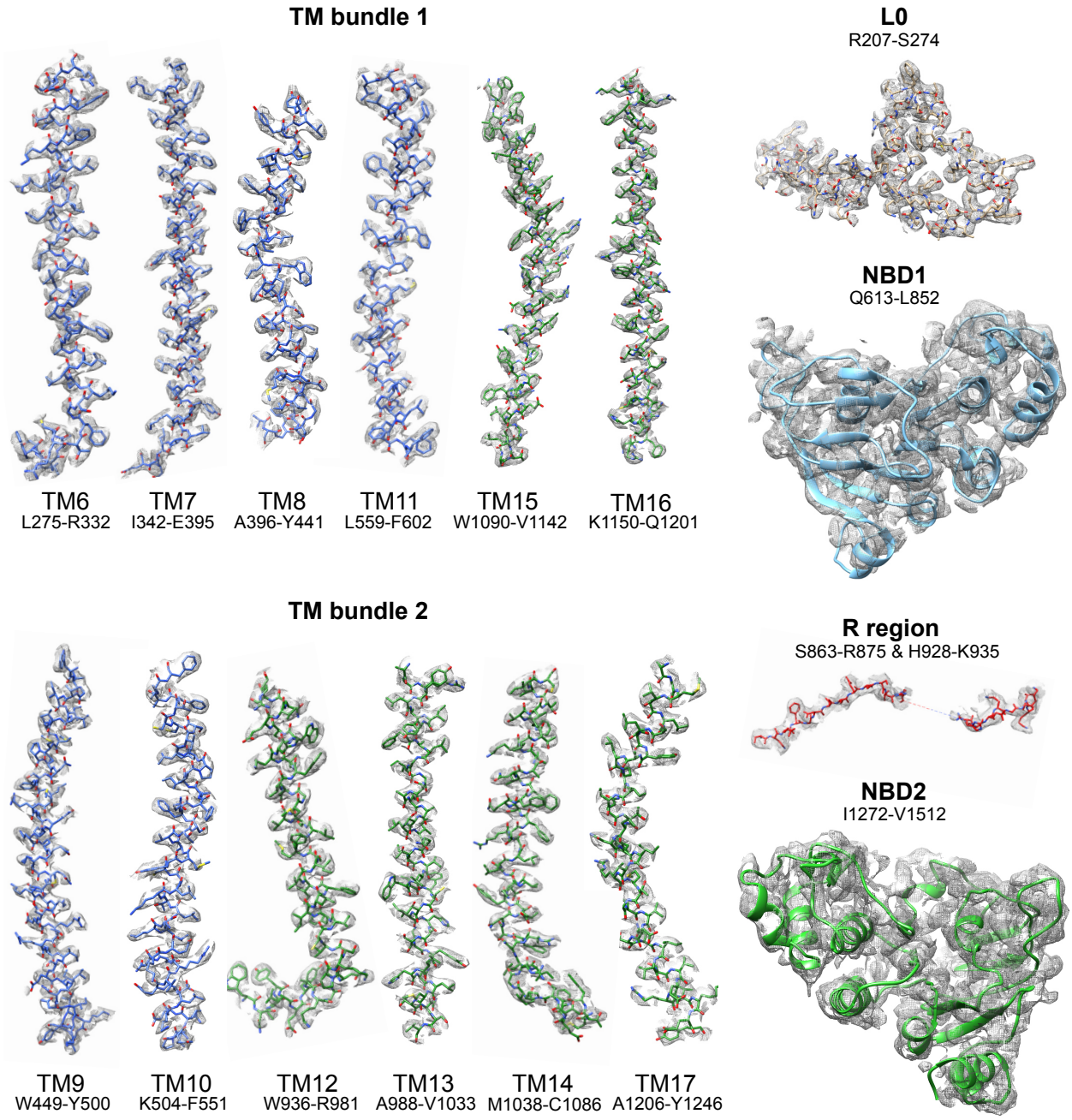

Fig. S5. Representative model-in-map fit for the L0 linker and ABC core of Ycf1p. Examples of the atomic model of Ycf1p fit into the experimental cryo- EM map are shown for individual transmembrane helices in TM bundles 1 and 2, the L0 linker, two segments of the R region, and NBD1 and NBD2.

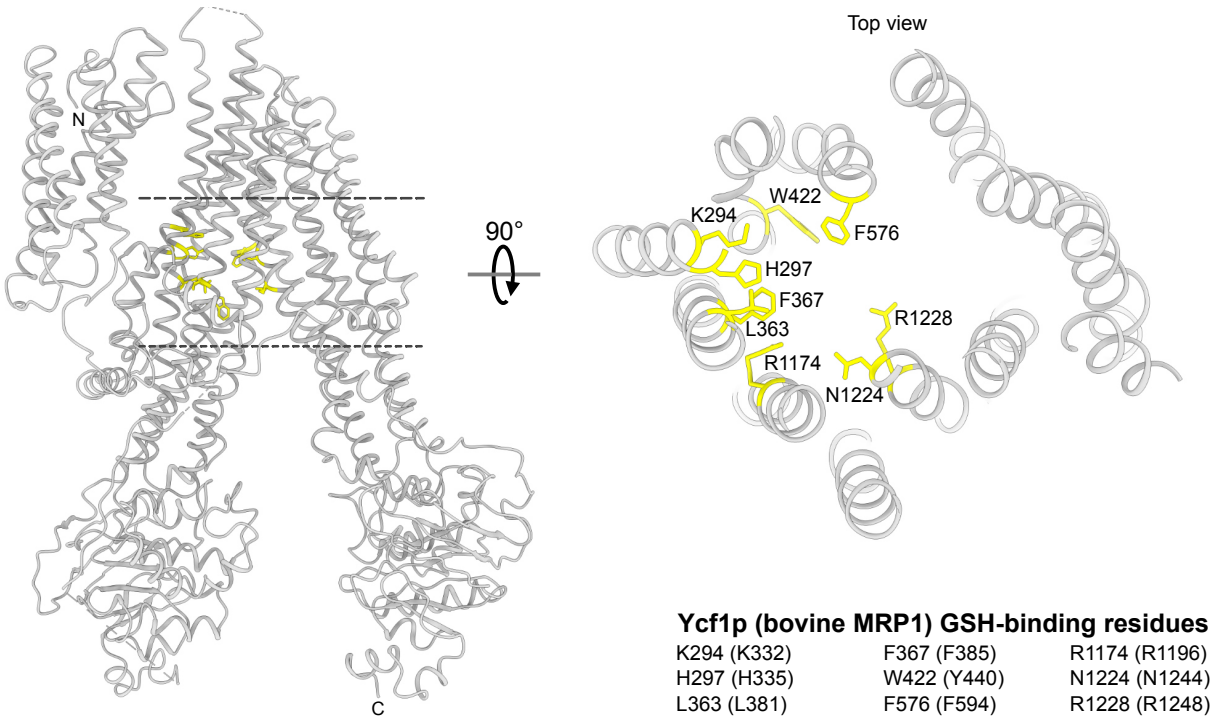

Fig. S6. Homologous bovine MRP1 GSH binding residues in Ycf1p. The identity of potential GSH-binding residues in Ycf1p, shown in yellow, are based on the structure of bovine MRP1 bound to substrate (1). Ycf1p residues that form the putative GSH-binding site are summarized in the table, with the homologous GSH-binding residues in bovine MRP1 indicated in brackets.

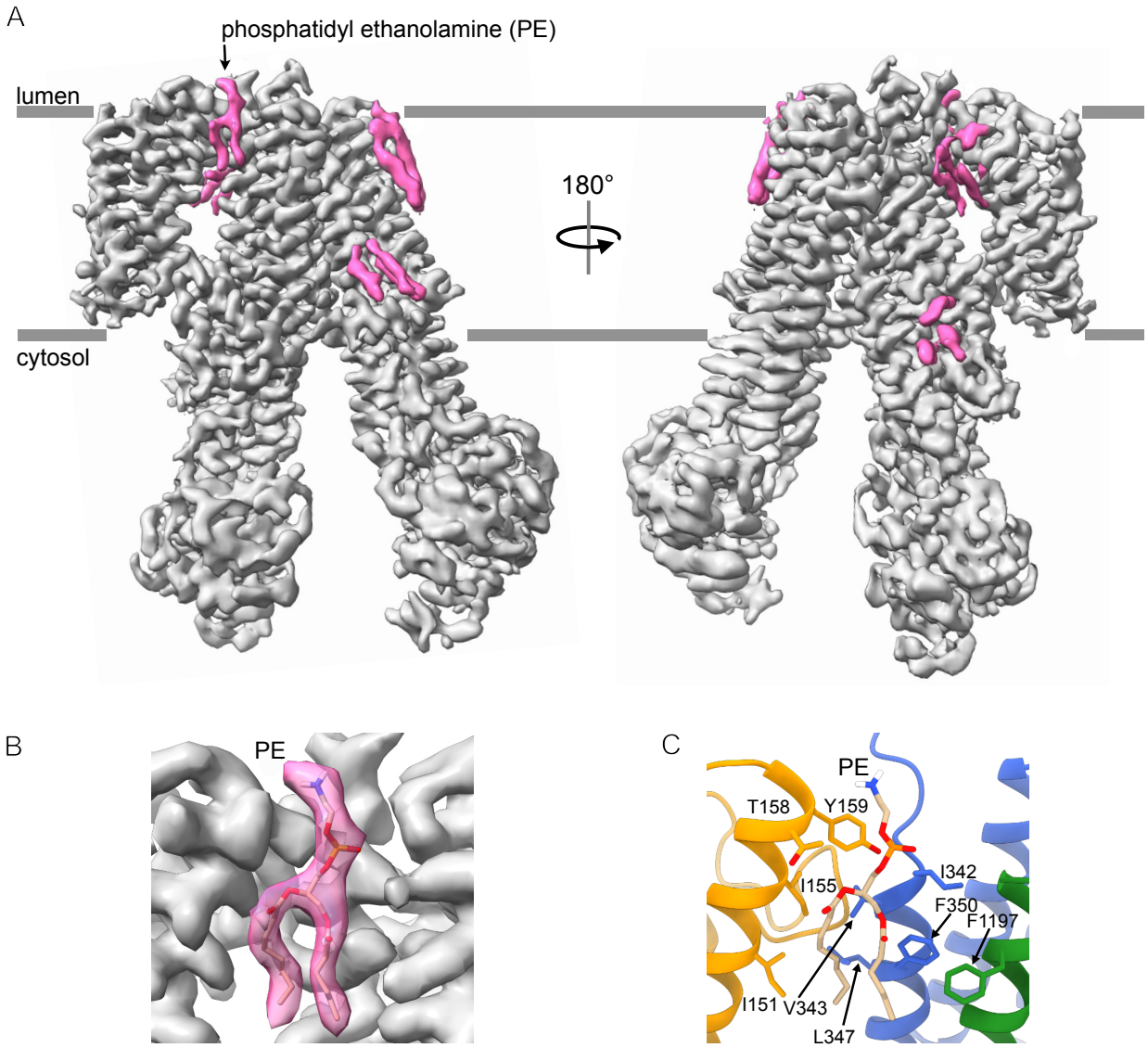

Fig. S7. Lipid densities in Ycf1p transmembrane region. (A) Cryo-EM map of Ycf1p with density corresponding to the protein in grey and density corresponding to lipid molecules in pink. The prominent phospholipid density at the TMD0/ABC core interface at luminal side membrane is modeled as phosphatidylethanolamine. (B) Fit of the phosphatidylethanolamine into the corresponding phospholipid density with the lipid tail truncated to fit the observed density. (C) Interactions of phosphatidylethanolamine with residues in TM4 (I151, T157, Y159), TM7 (I342, V343, F346, L347), and TM15 (F1197). The lipid is shown in tan, TMD0 is shown in orange, TMD1 is shown in blue, and TMD2 is shown in green.

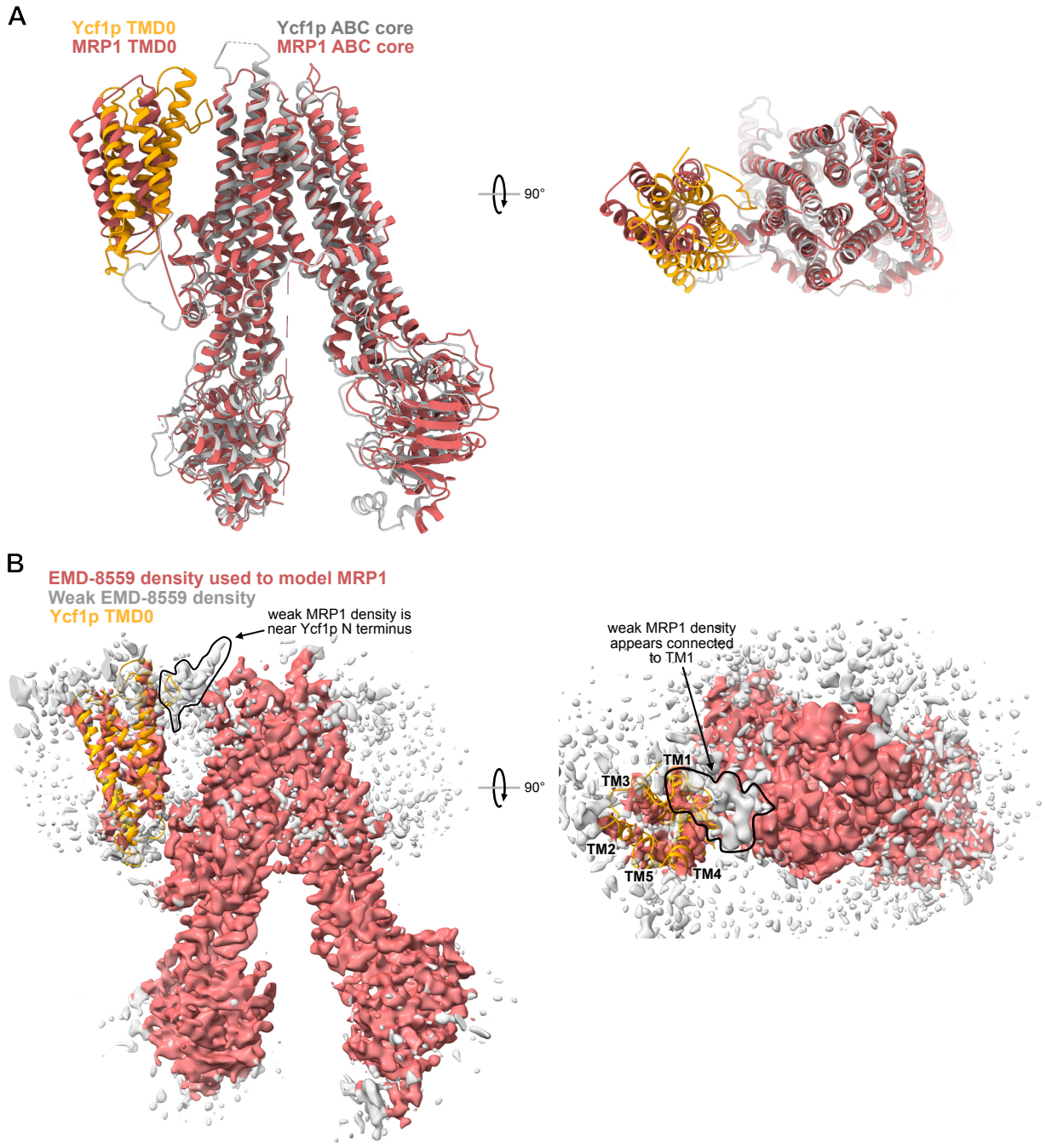

Fig. S8. Assignment of bovine MRP1 TMD0 helices and the unknown density at the interface between TMD0 and the ABC core extracellular interface based on the Ycf1p structure. (A) Overlay of the ABC core and L0 linker of Ycf1p and bovine MRP1 (R.M.S.D. 1.88 Å), showing that the TMD0 helix bundle of MRP1 projects away from the ABC core. The MRP1 structure is shown in red while Ycf1p TMD0 is in orange and both the Ycf1p L0 linker and ABC core are in grey. (B) The cryo-EM model of Ycf1p TMD0 (orange) can be fit into the MRP1 density (grey) revealing the topology of MRP1 TMD0. Notably, the region of weak density in the MRP1 map at the extracellular side of the membrane can be tentatively assigned to the N-terminal tail of MRP1.

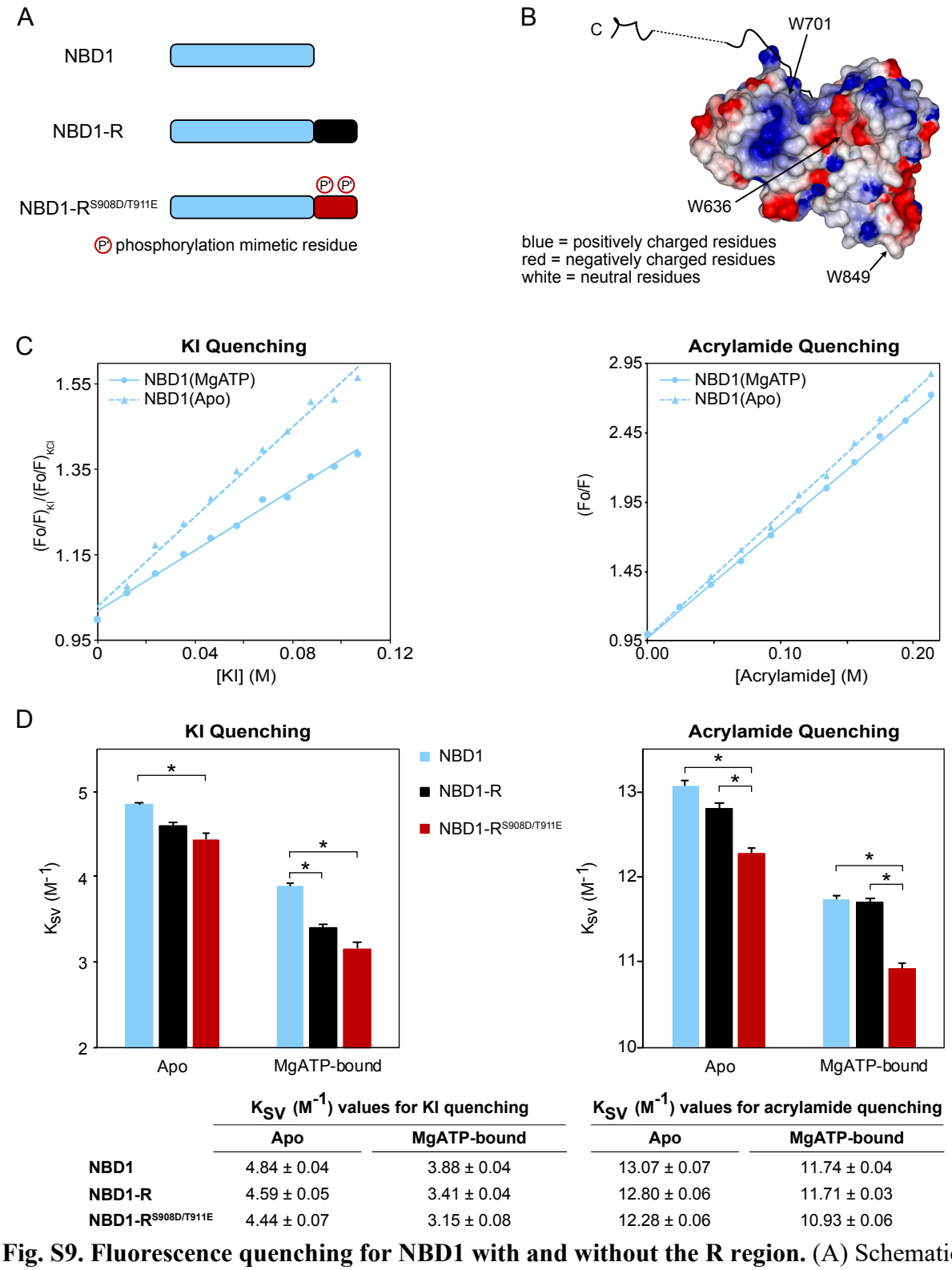

	K_{SV} (M^{-1}) values for KI quenching		K_{SV} (M^{-1}) values for acrylamide quenching	
	Apo	**MgATP-bound**	**Apo**	**MgATP-bound**
NBD1	4.84 ± 0.04	3.88 ± 0.04	13.07 ± 0.07	11.74 ± 0.04
NBD1-R	4.59 ± 0.05	3.41 ± 0.04	12.80 ± 0.06	11.71 ± 0.03
NBD1-R$^{S908D/T911E}$	4.44 ± 0.07	3.15 ± 0.08	12.28 ± 0.06	10.93 ± 0.06

Fig. S9. Fluorescence quenching for NBD1 with and without the R region. (A) Schematic representation of NBD1, NBD1-R, and NBD1-R$^{S908D/T911E}$. The R region is coloured red in NBD1-R$^{S908D/T911E}$, and is labeled with two circled P' in order to highlight the phosphorylation mimetic mutations. (B) Surface representation of NBD1 from the Ycf1p atomic model, with blue

and red representing positive and negative electrostatic potential, respectively, and white for neutral residues. The three Trp residues in NBD1 are labeled. The backbone traces of the observed segments R region are shown as solid black coils while a dotted black line denotes the unresolved R region segment. (C) Representative Stern-Volmer plots for I^- and acrylamide quenching of NBD1 in absence (blue triangles and dotted lines) and presence of adenosine triphosphate bound to an Mg^{2+} ion (MgATP; blue circles and solid lines lines). (D) Bar graph showing average K_{SV} values for I^- and acrylamide quenching of NBD1 (blue), NBD1-R (black), NBD1- $R^{S908D/T911E}$ (red). Error bars represent standard deviations from three independent measurements. Pairwise differences were examined with a t-test and the asterisks represent p-values of ≤ 0.001. The table reports the average Stern-Volmer constants (K_{SV}) ± s.d.

Table S1. Summary of data collection, image processing, and model statistics

Data Collection	**EMD-23932**
Electron microscope	Titan Krios G3
Camera	Falcon4
Voltage (kV)	300
Pixel size (Å)	1.03
Total exposure (e-/Å^2)	45
Exposure rate (e-/pixels/s)	5
Number of frames	30
Image Processing	**EMD-23932**
Particle collection and selection software	cryoSPARC Live
3D map classification and refinement software	cryoSPARC v2
Motion correction software	cryoSPARC v2
CTF estimation software	cryoSPARC v2
Number of movies used	4,084
Initial particle images selected (no.)	2,789,383
Particle images contributing to final map (no.)	124,864
Symmetry	C1
Global map resolution (Å)	3.2
Model Building	**PDB ID 7MPE**
Modelling and refinement software	Coot, Phenix
Number of residues built	1428
RMS bond length (Å)	0.005
RMS bond angle (º)	0.681
Ramachadran outliers (%)	0.0
Ramachadran allowed (%)	6.9
Ramachadran favoured (%)	93.1
Rotamer outliers (%)	0.0
All-atom clashscore	14.5
MolProbity score	2.11
EMRinger score	2.09

SI References

1. Z. L. Johnson, J. Chen, Structural Basis of Substrate Recognition by the Multidrug Resistance Protein MRP1. *Cell* **168**, 1075-1085.e1079 (2017).